scientific reports

Check for updates

OPEN

Dysregulation of STS in keratinocytes promotes calcium signaling and differentiation

Tae-Uk Kwon, Yeo-Jung Kwon, Hyemin Park, Yoon-ji Kang & Young-Jin Chun✉

Steroid sulfatase (STS) is a key enzyme for the desulfation of steroid sulfates, converting them into their biologically active forms. Notably, X-linked ichthyosis (XLI), a genetic disorder characterized by hyperkeratinization, arises as a direct result of STS deficiency. Keratinocyte differentiation is essential for proper keratinization. In this study, gene ontology analysis from STS-deficient mice revealed enhanced differentiation and upregulation of calcium-related signaling. Calcium plays a key role in regulating keratinocyte differentiation, with STS-deficient cells showing a marked increase in intracellular calcium influx. Additionally, these cells significantly upregulated calcium-sensing receptors (CasR), leading to elevated tyrosine phosphorylation, increased differentiation signaling, and the upregulation of early differentiation markers, including keratin 1 and keratin 10, as seen in HaCaT cells and mouse primary keratinocytes. Furthermore, STS inhibitors enhanced the expression of E-cadherin and terminal differentiation markers such as involucrin and loricrin. Due to increased calcium sensitivity, STS-deficient cells treated with calcium exhibited a significant upregulation of differentiation markers and reduced sensitivity to calcium chelation. Collectively, our findings demonstrate that reduced STS expression and inhibition of its activity enhance calcium responsiveness, induce CasR expression, and amplify calcium signaling, thereby promoting keratinocyte differentiation. These findings offer valuable insights into the mechanisms underlying STS deficiency-induced hyperkeratinization.

Keywords STS, XLI, RNA-seq, CasR, Calcium influx, Keratinocyte

Abbreviations

CasR	Calcium-sensing receptor
GO	Gene ontology
GSEA	Gene set enrichment analysis
PI3K	phosphoinositide 3-kinase
RNA-seq	RNA-sequencing
STS	Steroid sulfatase
TNF-α	Tumor necrosis factorα
XLI	X-linked ichthyosis

Steroid sulfatase (STS), an enzyme localized in the endoplasmic reticulum and found in varying amounts across nearly all tissues, desulfates steroid hormones such as cholesterol sulfate and dehydroepiandrosterone sulfate (DHEAS), converting them into their biologically active forms[1,2]. In skin tissue, STS is predominantly localized in the epidermis[1]. Dysregulation of STS has been linked to several skin conditions. For example, elevated plasma DHEAS levels are associated with conditions such as androgenetic alopecia and hirsutism[3]. Notably, STS deficiency is linked to X-linked ichthyosis (XLI), a congenital disorder characterized by abnormal keratinization, resulting in large, dark brown scaly patches and a thickened stratum corneum[1,2]. These symptoms are thought to result from the accumulation of cholesterol sulfate[1,2]. In normal epidermis, cholesterol sulfate is produced by cholesterol sulfotransferase (SULT2B1b) and undergoes desulfation in the outer layer to form a cholesterol sulfate cycle, which strongly regulates epidermal differentiation, barrier function, and desquamation[4]. However, in STS-deficient epidermis, cholesterol sulfate cannot be converted to cholesterol, disrupting the normal cholesterol sulfate cycle and causing impairments in epidermal differentiation and barrier function[1–4]. Nonetheless, the precise mechanism of keratinization due to STS deficiency has not yet been fully elucidated.

College of Pharmacy and Center for Metareceptome Research, Chung-Ang University, Seoul 06974, Republic of Korea. ✉email: yjchun@cau.ac.kr

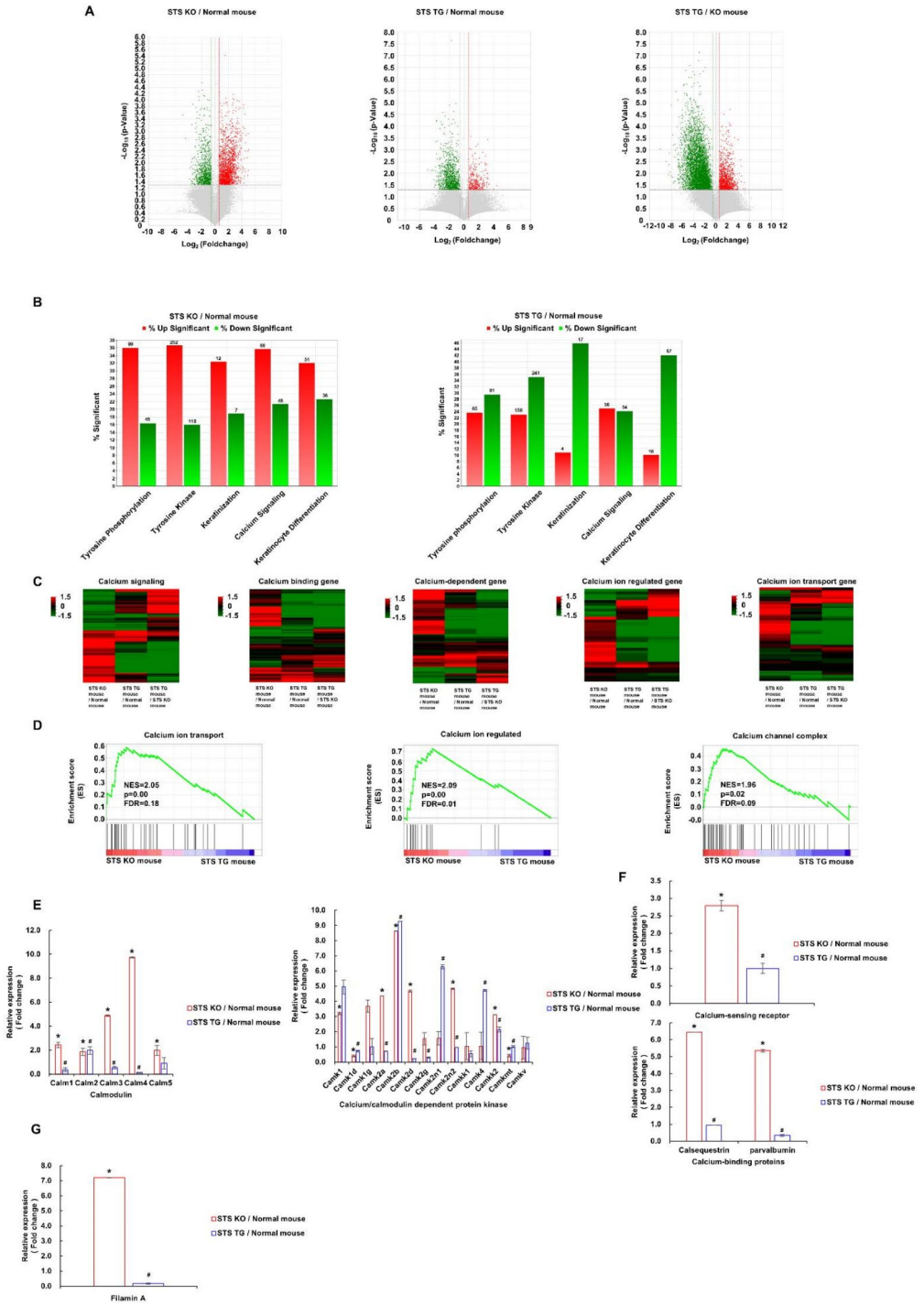

Thickening of the stratum corneum primarily occurs due to excessive keratinocyte differentiation and stratification, which weakens exfoliation by increasing cell cohesion[5–8]. Calcium is a key regulator of differentiation-related signaling pathways and plays a critical role in keratinocyte differentiation both in vivo and in vitro[9,10]. As keratinocytes move through the epidermal layers, calcium gradients drive their differentiation, forming the stratum corneum's barrier[10–14]. Changes in extracellular calcium concentrations activate calcium-sensing receptors (CasR) located in the plasma membrane, triggering intracellular signaling essential for differentiation[15]. Elevated calcium levels promote intercellular contact formation[16], and cadherins such as E-cadherin translocate to the membrane, facilitating the assembly of adherens junctions and desmosomes[17–20].

Upon calcium stimulation, E-cadherin binds to neighboring cells, while its cytoplasmic tail interacts with catenins to form the core of adherens junctions[21]. E-cadherin-mediated adhesion is essential for maintaining proper differentiation and remodeling cell-cell interactions[22,23]. Loss of E-cadherin disrupts adherens junctions

◀**Fig. 1**. STS deficiency enhances calcium signaling in mouse skin. Volcano plots, heat maps, and GSEA of RNA-seq data from STS KO, STS TG, and normal mouse skin. (**A**) Volcano plots showing DEGs in STS KO vs. normal, STS TG vs. normal, and STS TG vs. STS KO mouse skin. Upregulated genes are shown in red, downregulated genes in green. The fold-change threshold is set at 1.5, with a significance level of $p < 0.05$. (**B**) Gene ontology analysis of upregulated (red) and downregulated (green) gene clusters in STS KO and STS TG mouse skin. The numbers above the bars indicate the number of genes in each category. (**C**) Heatmaps depicting expression levels of genes related to calcium signaling, binding, dependency, ion regulation, and transport in STS KO, STS TG, and normal mouse skin. Expression levels are adjusted and normalized on a $\log_2$ scale. Upregulation and downregulation are indicated in red and green, respectively. (**D**) GSEA results revealing significant enrichment of calcium ion transport, calcium ion-regulated, and calcium channel complex genes in STS KO and STS TG mouse skin. (**E**) RNA-seq analysis of gene expression in calmodulins and calcium/calmodulin-dependent protein kinases. Data are presented as mean ± SD ($n = 3$). Statistical significance is indicated by $^{*,\#}p < 0.05$. (**F**) RNA-seq analysis of gene expression in calcium-sensing receptors and calcium-binding proteins. Data are presented as mean ± SD ($n = 3$). Statistical significance is indicated by $^{*,\#}p < 0.05$. (**G**) RNA-seq analysis of Filamin A gene expression. Data are presented as mean ± SD ($n = 3$). Statistical significance is indicated by $^{*,\#}p < 0.05$.

and impairs terminal differentiation[24]. Tyrosine phosphorylation also positively regulates cell adhesion during keratinocyte differentiation[17], and Src family kinases such as Src and Fyn exhibit elevated activity in calcium-differentiated keratinocytes[10,25,26].

CasR responds to extracellular calcium by triggering intracellular signaling cascades that drive differentiation[15]. As keratinocytes transition from growth to differentiation, they undergo proliferation, cell cycle arrest in the G_0/G_1 phase, and increased expression of early differentiation markers such as keratin 1 and keratin 10[5]. These markers play critical roles in regulating gene expression during both proliferation and differentiation[27,28]. Involucrin and loricrin, markers of terminal differentiation, are also important indicators of keratinocyte maturation[29,30], accumulating on the cytoplasmic side of the plasma membrane in keratinized cells[31–33].

In our previous work, we identified impaired cell motility and increased cell death as contributing factors to keratinization induced by STS deficiency[34]. To gain further insights into the underlying mechanisms of this phenomenon, we analyzed calcium signaling and differentiation factors using RNA-seq in STS-deficient and STS-overexpressing mouse models. Additionally, we modulated STS expression in keratinocytes to assess calcium influx, CasR levels, and differentiation markers. Therefore, this study provides a deeper understanding of the pathogenesis of skin diseases, such as XLI, caused by STS deficiency.

Results

STS deficiency amplifies calcium signaling in mouse skin tissue

RNA-seq analysis was conducted on skin tissue from STS knockout (KO) and transgenic (TG) mouse models (8-week-old males) to investigate the role of STS in the epidermis. Volcano plots representing approximately 39,000 gene expression levels were generated using a 1.5-fold cutoff for visualization (Fig. 1A). Using the Mouse Genome Informatics (MGI) database (https://www.informatics.jax.org/), we analyzed the effects of STS deficiency on keratinocyte differentiation. Gene ontology (GO) analysis revealed a significant upregulation of genes related to tyrosine phosphorylation, tyrosine kinase activity, keratinization, calcium signaling, and keratinocyte differentiation in STS KO mice compared to controls (Fig. 1B)[17,25,26,35]. In contrast, these genes were notably downregulated in STS TG mice (Fig. 1B).

We further identified genes involved in calcium signaling and generated a heatmap that showed a significant upregulation of calcium-related genes in STS KO mice (Fig. 1C, Table S1). These genes regulate calcium binding, dependence, ion regulation, and transport. Gene set enrichment analysis (GSEA) also revealed an upregulation of factors involved in calcium ion transport and regulation in STS KO mice compared to STS TG mice (Fig. 1D). RNA-seq data indicated elevated expression of calmodulin and calcium/calmodulin-dependent protein kinases, which regulate intracellular calcium levels, in STS KO mice (Fig. 1E)[36,37]. Furthermore, STS deficiency increased the expression of CasR and calcium-binding proteins such as calsequestrin and parvalbumin in STS KO mice (Fig. 1F)[38]. We also observed a significant increase in filamin A expression, which stabilizes CasR (Fig. 1G)[39]. These results suggest that STS deficiency enhances calcium signaling, leading to significant changes in keratinocyte differentiation.

STS deficiency increases intracellular calcium influx and upregulates CasR expression

To further validate the increase in calcium signaling observed in Fig. 1, we assessed calcium levels in STS-deficient and overexpressing cells. Confocal microscopy revealed higher calcium content in STS-deficient cells, while STS overexpression reduced calcium influx (Fig. 2A). Additionally, STS-deficient cells exhibited greater calcium influx when cultured in a high-calcium medium compared to controls. Treatment with the calcium chelator BAPTA-AM[40] reduced this influx, albeit to a lesser extent in STS-deficient cells (Fig. 2B). These results suggest that inhibiting STS enhances intracellular calcium influx and may activate calcium signaling.

Next, we examined CasR expression, a key regulator of calcium homeostasis. RNA-seq analysis confirmed the upregulation of CasR in STS KO mice (Fig. 1G), a pattern also observed in STS-deficient keratinocytes (Fig. 2C, D). Treatment with STX-64, an STS inhibitor[41,42], led to a dose-dependent increase in CasR expression (Fig. 2E, F). These findings indicate that the upregulation of CasR following STS inhibition contributes to the enhanced intracellular calcium influx.

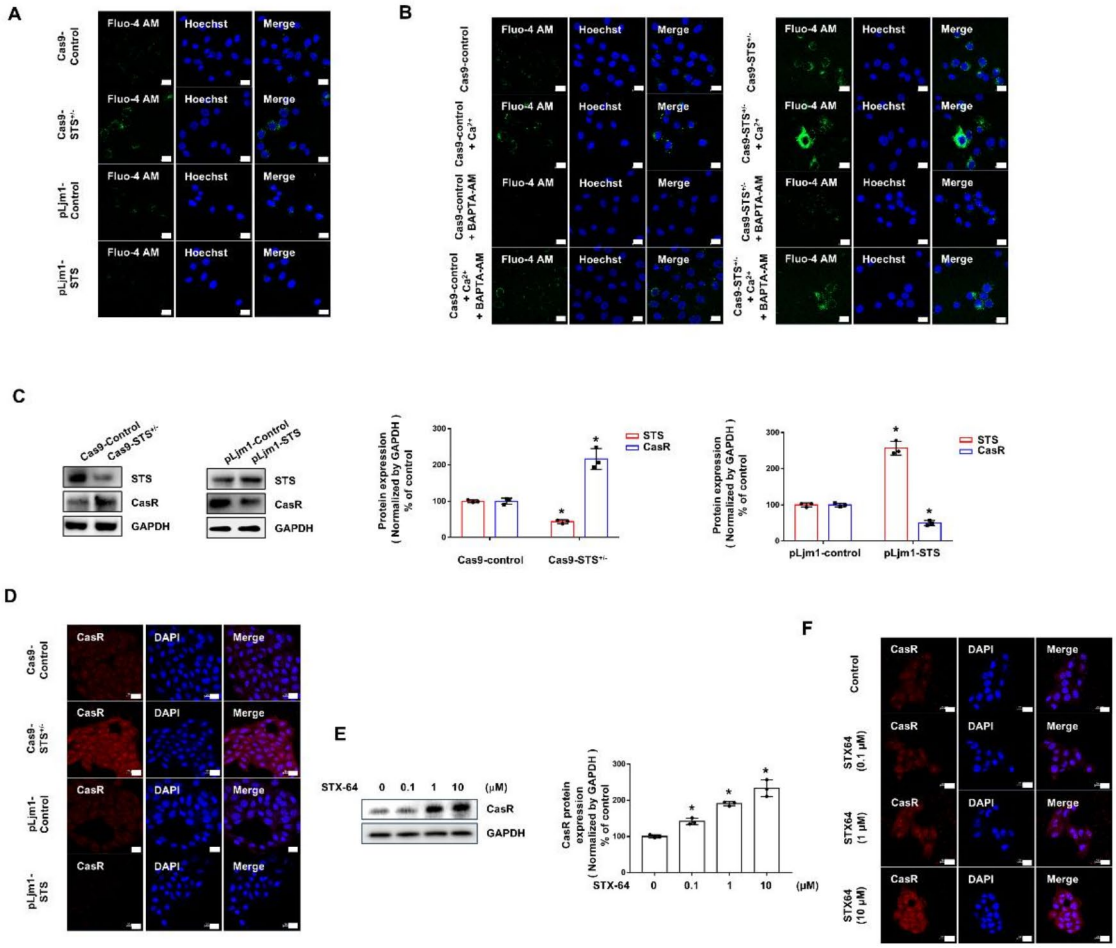

Fig. 2. Reduced STS expression in keratinocytes increases intracellular calcium influx and upregulates CasR (**A**) Representative confocal microscopy images of Cas9- and pLJM1-HaCaT cells. Intracellular calcium was stained with Fluo-4 AM (green), and nuclei were stained with Hoechst-33,258 (blue). Scale bar = 20 μm. (**B**) Representative confocal microscopy images of Cas9-HaCaT cells treated with calcium (140 nM) and BAPTA-AM (5 μM). Intracellular calcium was stained with Fluo-4 AM (green), and nuclei were stained with Hoechst-33,258 (blue). Scale bar = 20 μm. (**C**) Western blot analysis of total cellular protein (20 μg) from Cas9- and pLJM1-HaCaT cells, with GAPDH as a loading control. The blot shows STS and CasR protein levels. Data are expressed as mean ± SEM of three experiments. $^{*}p < 0.05$ compared to the control. (**D**, **F**) Immunofluorescence staining of CasR. Cells were fixed, incubated with CasR antibodies, and stained with Alexa Fluor 594-labeled secondary antibody. Images were captured using fluorescence microscopy. Blue = DAPI; scale bar = 20 μm. (**D**) Representative immunofluorescence images showing CasR expression in Cas9- or pLJM1-HaCaT cells. (**E**, **F**) HaCaT cells treated with STX-64 (0, 0.1, 1, or 10 μM) for 48 h. (**E**) Western blot analysis of total cellular protein (20 μg) showing CasR protein levels in HaCaT cells, with GAPDH as a loading control. (**F**) Representative immunofluorescence images of CasR expression in HaCaT cells.

STS deficiency enhances keratinocyte early differentiation in both mouse skin and cultured keratinocytes

We investigated the effects of enhanced calcium signaling on keratinocyte differentiation resulting from STS suppression. RNA-seq data revealed an upregulation of genes related to tyrosine kinase activity and tyrosine phosphorylation, which promote differentiation, in STS KO mice compared to controls, while genes related to tyrosine phosphatase activity were downregulated (Fig. 3A, Table S2). Additionally, genes involved in keratinocyte differentiation and keratinization were significantly upregulated (Fig. 3B, Table S3). Calcium-induced keratinocyte differentiation requires phosphoinositide 3-kinase (PI3K) activation[16], and RNA-seq data confirmed increased expression of PI3K subunits, including PIK3CA and PIK3CB, in STS-deficient mice (Fig. 3C).

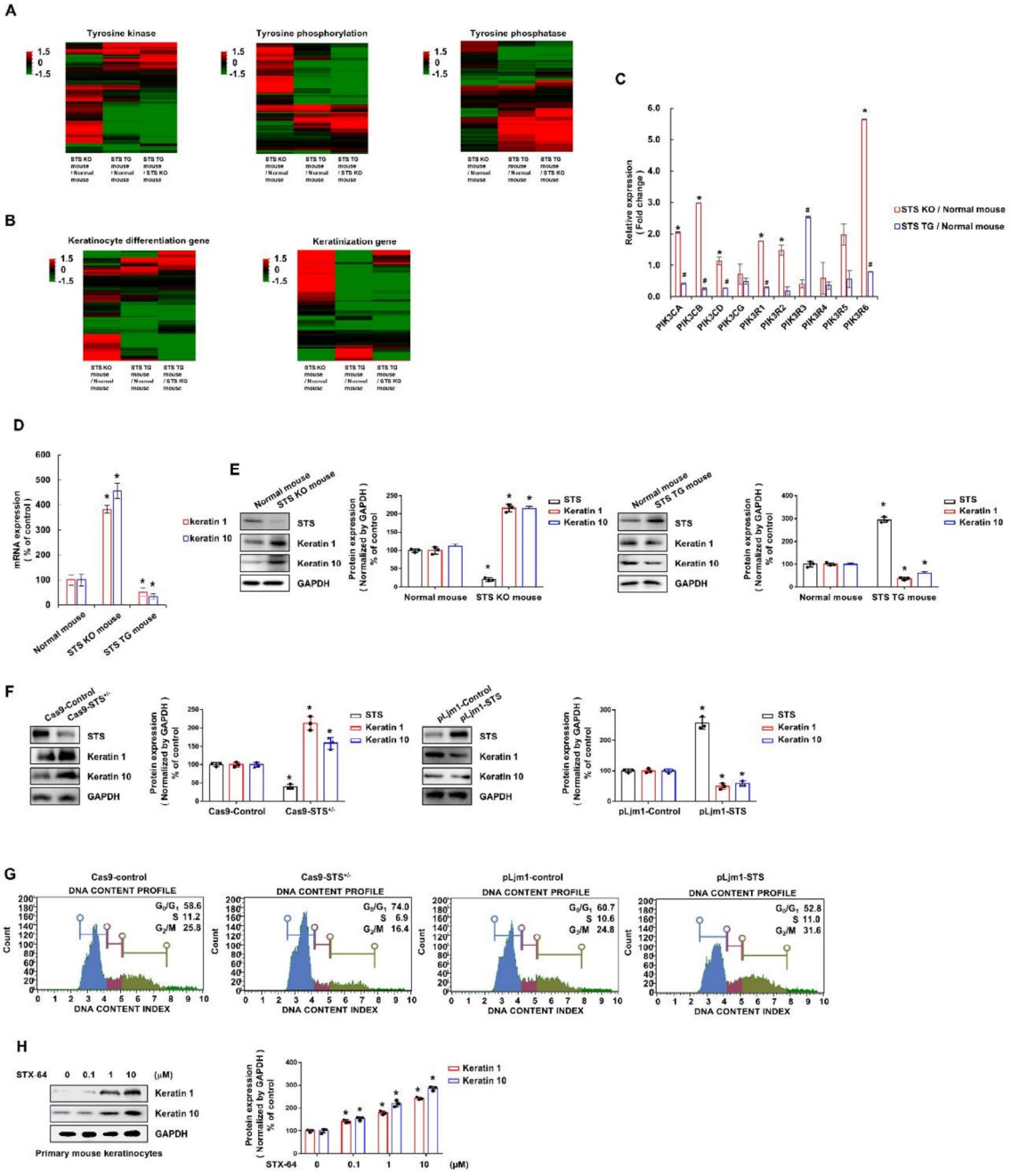

Fig. 3. Suppression of STS expression promotes differentiation of keratinocytes. (**A**) Heatmaps showing the expression of tyrosine kinase, tyrosine phosphorylation, and tyrosine phosphatase-related genes in STS KO, STS TG, and normal mouse skin. (**B**) Heatmaps of keratinocyte differentiation and keratinization genes in STS KO, STS TG, and normal mouse skin. (**C**) RNA-seq analysis of gene expression in PI3K subunits. Data are expressed as mean ± SD ($n = 3$). $^{*,\#}p < 0.05$. (**D**) Real-time qPCR analysis of mRNA expression levels for keratin 1, and keratin 10 in STS KO and STS TG mouse skin tissues. Data are expressed as mean ± SEM of three experiments. $^{*}p < 0.05$ compared to the control. (**E**, **F**, **H**) Representative western blot image showing STS, keratin 1, and keratin 10 protein levels with GAPDH as a loading control. Data are presented as mean ± SEM of three experiments. $^{*}p < 0.05$ compared to the control. (**E**) Western blot analysis of total cellular protein (40 μg) in STS KO, STS TG, and normal mouse skin (**F**) Western blot analysis of total cellular protein (20 μg) in Cas9-STS$^{+/-}$ and pLJM1-STS HaCaT cells. (**G**) Cell cycle distribution was measured using a Muse cell cycle kit. Data are presented as mean ± SD ($n = 3$). (**H**) Primary mouse keratinocytes treated with STX-64 (0, 0.1, 1, or 10 μM) for 48 h. Western blot analysis of total cellular protein (20 μg) with GAPDH as a loading control.

mRNA levels of early differentiation markers, including keratin 1 and keratin 10, were significantly upregulated (Fig. 3D), and protein levels were similarly elevated in STS-deficient mouse skin tissue (Fig. 3E). In cell experiments, standard calcium concentrations were used to focus solely on the effects of STS. Under these conditions, STS-deficient and STS-overexpressing HaCaT cells showed a similar upregulation in the expression of early differentiation markers, consistent with the results observed in STS-deficient mouse skin tissue (Fig. 3F). We then analyzed STS-deficient and STS-overexpressing cells to assess the impact of STS suppression on keratinocyte differentiation, which typically occurs during the G_0/G_1 phase[10]. STS-deficient cells exhibited G_0/G_1 arrest (Fig. 3G). Additionally, treatment of primary cells with STX-64 at concentrations of 0, 0.1, 1, or 10 μM resulted in a dose-dependent increase in keratin 1 and keratin 10 expression (Fig. 3H). These findings suggest that STS reduction enhances early keratinocyte differentiation, thereby increasing the structural stability of the epidermis.

Increased calcium responsiveness in STS-deficient keratinocytes elevates the expression of terminal differentiation markers

We assessed the expression of E-cadherin and the terminal differentiation markers involucrin and loricrin, which play key roles in keratinocyte differentiation[6,29,32]. Inhibiting STS activity significantly increased their expression in HaCaT cells treated with STX-64 (Fig. 4A, B), with a similar pattern observed in STS-overexpressing cells (Fig. 4C, D). Conversely, treatment with TNF-α, a known inducer of STS[1,4], reduced the expression of these markers as STS levels increased in HaCaT or STS-overexpressing cells (Fig. 4E, F). This upregulation of E-cadherin and terminal differentiation markers was also observed in mouse primary keratinocytes treated with STX-64 (Fig. 4G, H), indicating that reducing STS affects both early and late stages of keratinocyte differentiation (Figs. 3 and 4).

Furthermore, we analyzed the expression of E-cadherin, involucrin, and loricrin in response to calcium treatment in keratinocytes. The expression of these factors increased in a calcium concentration-dependent manner (Fig. 5A). Calcium treatment significantly upregulated all markers in STS-deficient cells, with E-cadherin and involucrin levels increasing by 5.7- and 7.1-fold, respectively, compared to controls. These markers were less sensitive to BAPTA-AM-induced calcium suppression, showing only a 32.3% and 21.2% decrease, respectively. Co-treatment with BAPTA-AM and calcium restored their expression to levels similar to those seen in untreated STS-deficient cells (Fig. 5B). In contrast, calcium treatment in STS-overexpressing cells increased E-cadherin, involucrin, and loricrin expression by 1.85- to 2.36-fold, but this increase was smaller compared to STS-deficient cells (Fig. 5C). Overall, STS inhibition significantly enhanced responsiveness to calcium, leading to upregulated expression of E-cadherin, involucrin, and loricrin.

Discussion

Our study used RNA-seq data from STS KO and TG mouse models to investigate the impact of STS deficiency on skin diseases, particularly XLI (Fig. 1A,B). We focused on genes and signaling pathways involved in keratinocyte differentiation, given the abnormal keratinization observed in XLI[1,2]. Our findings demonstrate that STS deficiency amplifies calcium signaling and accelerates keratinocyte differentiation, likely contributing to the abnormal keratinization seen in skin conditions such as XLI. These insights provide a deeper understanding of the role of STS deficiency in the pathogenesis of skin disorders.

Calcium is a crucial factor in keratinocyte differentiation[9,10], and patients with XLI have been shown to exhibit elevated calcium levels in the stratum corneum[5]. Our study confirmed that STS deficiency intensifies calcium signaling in mouse skin. RNA-seq analysis revealed a significant upregulation of genes related to calcium signaling, binding, and ion transport in STS-deficient mice (Fig. 1C–G). This finding aligns with the increased intracellular calcium levels observed in STS-deficient keratinocytes (Fig. 2A,B), further supporting the key role of calcium as a regulator of keratinocyte differentiation and skin barrier formation. The heightened calcium signaling in STS KO mice likely drives excessive keratinocyte differentiation, contributing to impaired keratinization.

Additionally, STS-deficient keratinocytes showed increased expression of CasR (Fig. 2C–F), supporting the hypothesis that STS modulates calcium homeostasis. CasR regulates extracellular calcium and triggers calcium-dependent signaling within keratinocytes, promoting calcium influx[15,43]. These findings suggest that STS deficiency upregulates CasR, resulting in increased intracellular calcium influx and enhanced calcium signaling. However, further research is needed to clarify the mechanisms by which STS regulates CasR expression.

Furthermore, a recent study using RNA-seq data from siRNA-based reduction of STS expression in human primary keratinocytes showed an enrichment of genes involved in cell-substrate junction assembly[45]. STS deficiency also enriched genes related to tyrosine kinases and phosphorylation, which are key drivers of differentiation and cell adhesion during calcium-induced keratinocyte differentiation (Fig. 3A). Genes involved in keratinocyte differentiation and keratinization were similarly upregulated (Fig. 3B,C), showing increased expression of E-cadherin, keratin 1, keratin 10, involucrin, and loricrin (Figs. 3D–H and 4). E-cadherin plays a crucial role in mediating calcium-induced cell adhesion and promoting keratinocyte differentiation[44,45]. The enhanced expression of E-cadherin, alongside its role in cell-cell adhesion, suggests that STS may influence keratinocyte differentiation and adhesion through calcium signaling.

Several studies have examined the interactions between CasR, filamin A, and E-cadherin[16,39,45]. Extracellular calcium induces differentiation by activating CasR-mediated signaling and E-cadherin-mediated adhesion[16]. The sequential binding of catenins such as E-cadherin to the cytoskeleton and other signaling molecules, including PI3K[22,46]. PI3K activation is essential for calcium-induced keratinocyte differentiation, and CasR has been shown to regulate the E-cadherin/PI3K pathway via Src family kinases[16]. The increased expression of PI3K observed in STS KO mice is consistent with this regulatory pathway (Fig. 3C). Additionally, STS-deficient keratinocytes demonstrated heightened sensitivity to calcium, along with a significant increase in differentiation

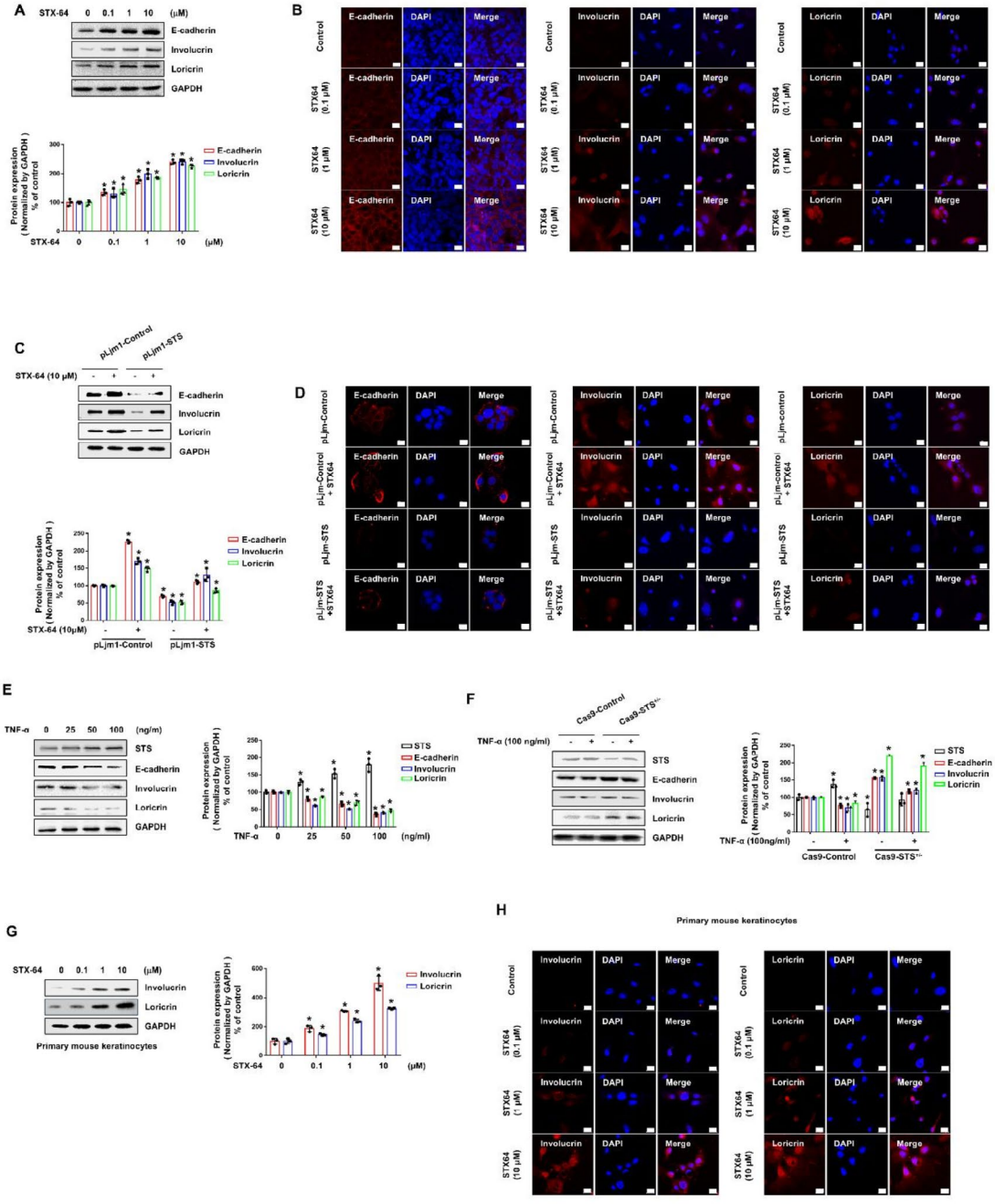

Fig. 4. Inhibition of STS activity upregulates the expression of E-cadherin, involucrin, and loricrin in keratinocytes. **(A, C, E-G)** Western blot analysis of total cellular protein (20 μg), with GAPDH as a loading control. Data are presented as mean ± SEM of three experiments. $^{*}p < 0.05$ compared to the control. **(A, C)** Representative western blot images showing E-cadherin, involucrin, and loricrin protein levels. **(A, B)** HaCaT cells were treated with STX-64 (0, 0.1, 1, or 10 μM) for 48 h. **(B, D)** Immunofluorescence staining was conducted. Cells were fixed, incubated with antibodies against E-cadherin, involucrin, and loricrin, and stained with Alexa Fluor 594-labeled secondary antibody. Images were captured using fluorescence microscopy. Blue = DAPI; scale bar = 20 μm. **(C, D)** pLJM1-HaCaT cells were treated with STX-64 (0 or 10 μM) for 48 h. **(D)** Representative immunofluorescence images showing E-cadherin, involucrin, and loricrin expression in Cas9 or pLJM1-HaCaT cells. **(E, F)** Representative western blot images showing STS, E-cadherin, involucrin, and loricrin protein levels. **(E)** HaCaT cells treated with TNF-α (0, 25, 50, or 100 ng/ml) for 48 h. **(F)** Cas9-HaCaT cells treated with TNF-α (0 or 100 ng/ml) for 48 h.

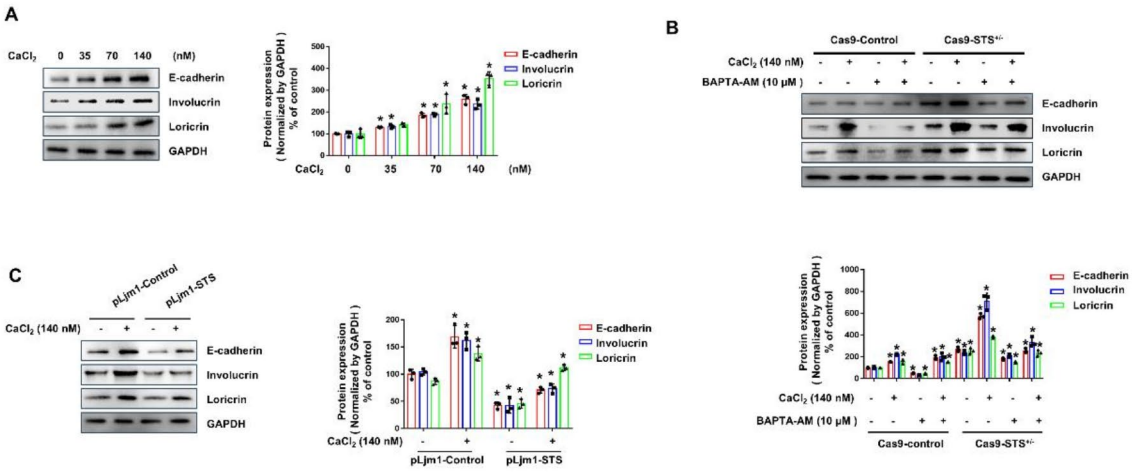

Fig. 5. Calcium significantly increases differentiation marker expression in STS-deficient keratinocytes. (**A**–**C**) Representative western blot images of E-cadherin, involucrin, and loricrin expressions in (**A**) HaCaT cells treated with Ca^{2+} (0, 35, 70, or 140 nM) for 48 h, (**B**) Cas9-HaCaT cells treated with Ca^{2+} (0 or 140 nM), or BAPT-AM (0 or 5μM) for 48 h, and (**C**) pLjm1-HaCaT cells treated with Ca^{2+} (0 or 140 nM) for 48 h. Western blot analysis was performed on total cellular protein (20 μg), with GAPDH serving as a loading control. Data are shown as mean ± SEM of three experiments. $^{*}p < 0.05$ compared to the control.

markers. Thus, STS deficiency not only upregulates E-cadherin expression but also strengthens E-cadherin-mediated adhesion in response to external calcium, potentially leading to dysregulation of the differentiation process.

In summary, STS plays a key role in regulating calcium signaling and keratinocyte differentiation. STS deficiency increases intracellular calcium influx and signaling, driving the expression of crucial differentiation markers (Fig. 6). These findings offer valuable insights into the mechanisms underlying STS deficiency-related skin disorders, such as XLI, and suggest potential therapeutic strategies that target calcium signaling modulation.

Materials and methods

Cell culture

HaCaT, a human keratinocyte cell line, was obtained from CLS Cell Lines Service (Germany). HaCaT, pLjm1-Control HaCaT, and pLjm1-STS HaCaT cells were cultured in Dulbecco's Modified Eagle Medium (DMEM) supplemented with 10% (v/v) fetal bovine serum (FBS), 100 U/mL penicillin, and 100 μg/mL streptomycin. Cas9-control HaCaT and Cas9-STS$^{+/-}$ HaCaT cell lines were grown in DMEM with 20% (v/v) FBS, along with the same concentrations of penicillin and streptomycin. All cell lines were incubated at 37 °C in a humidified atmosphere containing 5% CO_2. After 24 h of incubation, cells were treated with TNF-α or STX-64 for either 24–48 h.

Reagents

STX-64 and Ultra Cruz™ mounting medium (sc-24941) were purchased from Santa Cruz Biotechnology (Dallas, TX). TNF-α and MG132 were purchased from Enzo Biochem (Farmingdale, NY), and $CaCl_2$, and cycloheximide from Sigma-Aldrich (Burlington, MA). DMEM was obtained from HyClone (Logan, UT), while Fluo-4 AM was acquired from Glpbio (California, CA). FBS and charcoal-stripped FBS were supplied by Tissue Culture Biologicals (Long Beach, CA). The Neon™ Transfection System, BAPTA-AM, and Hoechst 33,258 were procured from Thermo Fisher Scientific (Waltham, MA), and the D-Plus™ ECL solution from Dongin LS (Seoul, Korea). Except for TNF-α (dissolved in triple-distilled water), all chemicals were prepared in dimethylsulfoxide (DMSO), stored in small aliquots at −20 °C, and diluted in cell culture media prior to use. The following antibodies were used in our experiments: anti-STS polyclonal antibody (ab62219), involucrin antibody (ab53112), and loricrin antibody (ab85679) from Abcam (Cambridge, MA); cytokeratin 1 antibody (ab93652) and cytokeratin 10 antibody (ab76318) from Proteintech (Rosemont, IL); goat anti-rabbit IgG-Texas Red antibody (sc-2780) and CaSR antibody (6D4) from Santa Cruz Biotechnology (Santa Cruz, CA); E-cadherin antibody (07-697) from Merck Millipore (Burlington, MA); and GAPDH antibody from Cusabio Technology (Houston, TX). All other chemicals were sourced from commercial suppliers.

Stable transfection

The STS coding sequence was cloned into the pcDNA3.1/Zeo + vector for transient transfection experiments. For lentiviral production, the plasmid vectors pLJM1-Empty (provided by Joshua Mendell, Addgene plasmid

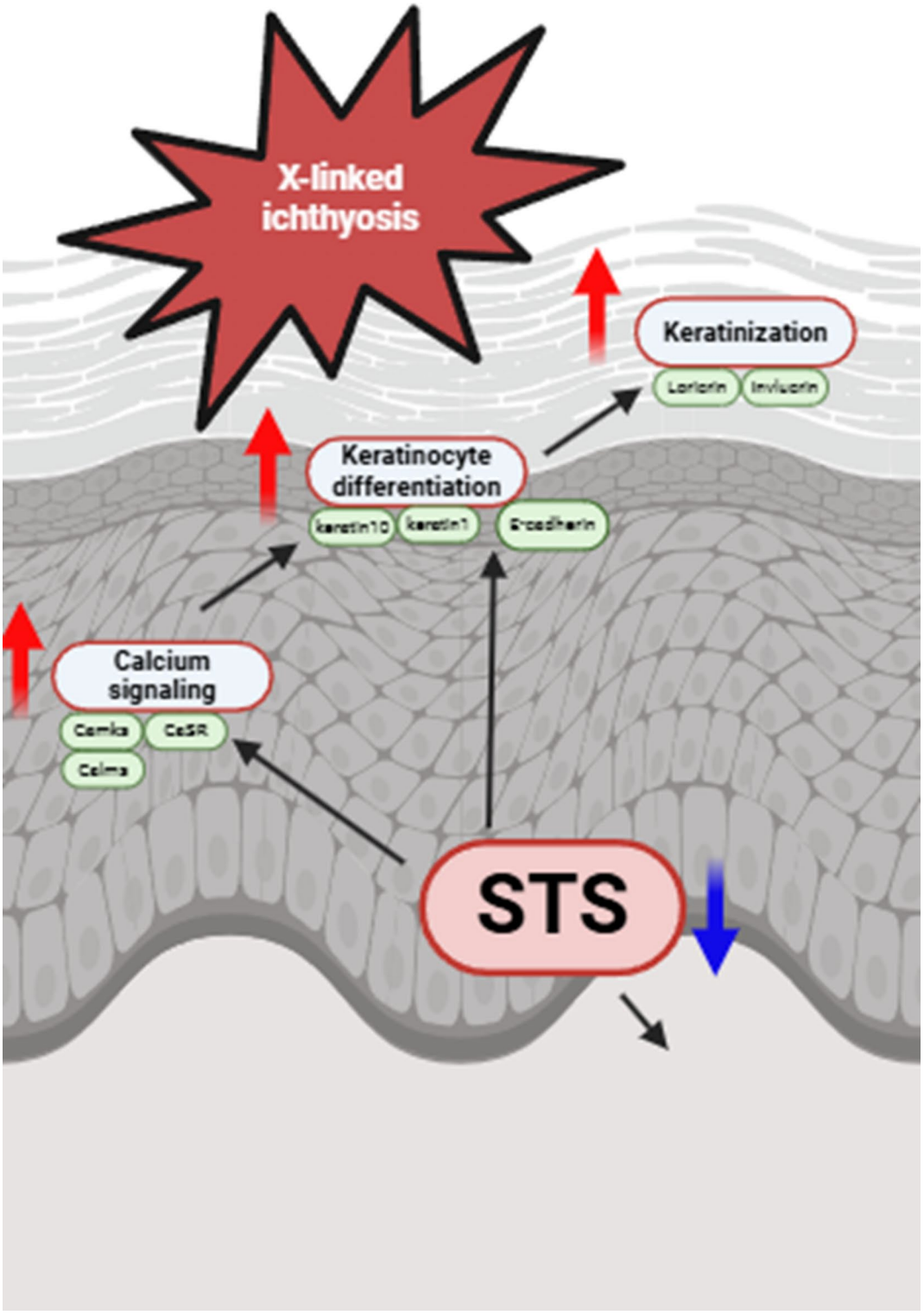

Fig. 6. Dysregulation of STS contributes to skin disorders such as XLI, characterized by abnormal keratinization. This study used STS-deficient mouse and cell models to show that STS inhibition enhances calcium signaling and keratinocyte differentiation. These findings offer insights into the mechanisms behind hyperkeratinization associated with STS deficiency.

#91980), pLKO.1 puro (provided by Bob Weinberg, Addgene plasmid #8453), pMD2.G, and psPAX2 (provided by Didier Trono, Addgene plasmids #12259 and #12260) were utilized. HEK293T cells were co-transfected with pLJM1-STS, pMD2.G, and psPAX2. After 48 h, the lentiviral supernatant containing the STS gene was collected and used to infect HaCaT cells in the presence of polybrene (8 μg/mL) for 24 h. HaCaT cells stably overexpressing STS were selected with puromycin (1 μg/mL).

Generation of Cas9-STS$^{+/-}$ HaCaT cells

The plasmid vectors pLentiCas9-T2A-GFP (Addgene plasmid #78548, a gift from Roderic Guigo and Rory Johnson) and tet-pLKO-sgRNA-puro (Addgene plasmid #104321, a gift from Nathanael Gray) were obtained from Addgene. Lentiviral supernatants containing either the Cas9 gene or STS-specific sgRNA were generated using HEK293T cells. Cas9-STS$^{+/-}$ HaCaT cells were then isolated through single-cell cloning into 96-well plates.

Quantitative reverse transcription PCR (RT-qPCR)

RT-qPCR analysis was performed using the Rotor-Gene Q system (Qiagen, Netherlands) with data processed using the QIAGEN Rotor-Gene Q Series software. Each RT-qPCR reaction mixture consisted of 10 μL of Q Green 2× qPCR Master Mix, 1 μM of specific oligonucleotide primers, and 20 ng of cDNA, totaling a volume of 20 μL. The amplification protocol included an initial denaturation at 95 °C for 5 min, followed by 40 cycles of denaturation at 95 °C for 15 s and annealing/extension at 56 °C for 45 s. The following primer sets were used for RT-qPCR: **18 S rRNA**: 5′-GTA ACC CGT TGA ACC CCA TT-3′ and 5′-CCA TCC AAT CGG TAG TAG CG-3′; **Keratin 1 (mouse)**: 5′- GAG CAG ATC AAG TCA CTC AAT GA -3′ and 5′- CCC ATT TGG TTT GTA GCA CCT −3′; **Keratin 10 (mouse)**: 5′- GCC TCC TAC ATG GAC AAA GTC −3′ and 5′- GCC TCC TAC ATG GAC AAA GTC −3′.

Western blotting analysis

Cells and mouse skin samples were lysed in ice-cold PE buffer containing 50 mM NaF. The protein lysates were separated by SDS-PAGE on 8, 10, or 15% polyacrylamide gels and then transferred onto 0.45 μm PVDF membranes via electrophoresis. Membranes were blocked for 2 h at 4 °C with 5% (w/v) bovine serum albumin (BSA) in Tris-buffered saline containing 0.1% Tween-20 (TBST). Following blocking, the membranes were incubated with primary antibodies diluted 1:1000 in TBST. After primary antibody incubation, the membranes were treated with secondary antibodies for 2 h. Protein bands were visualized using D-Plus™ ECL solution (Dongin LS, Korea) and analyzed on a ChemiDoc XRS system (Bio-Rad, CA).

Immunofluorescence

Samples were fixed in 10% neutral formalin for 30 min at room temperature (24 °C), then blocked for 45 min in PBS containing 10% goat serum and 0.2% Triton X-100. After blocking, the samples were incubated overnight at 4 °C with a primary antibody diluted at a 1:200 ratio. The following day, they were treated with goat anti-rabbit IgG conjugated to Alexa Fluor 594 (1:200) for overnight staining. After three washes with PBS, coverslips were mounted on glass slides using Ultra Cruz™ mounting medium. Fluorescence signals were visualized using a confocal laser scanning microscope (LSM 800, Carl Zeiss, Germany).

Ethics statement

The wild-type mice used in this study were procured from Orient Bio and Lab Animal (Korea), while the genetically engineered mice were produced by Macrogen (Korea), and the study complies with all relevant ethical regulations. All animal experiments were approved by the Institutional Animal Care and Use Committee (IACUC) of Chung-Ang University (protocol numbers 2017-00096 and 2019-00003) and were reviewed and conducted in accordance with approved guidelines. All animal experiment reporting complies with the ARRIVE (Animal Research: Reporting of In Vivo Experiments) guidelines. Experimental mice were bred and maintained in the clean animal facility of Chung-Ang University. Two to three mice were housed per cage and maintained at 20 to 24 °C with a 12-hour light/dark cycle. Food and water were provided ad libitum to all mice. Room temperature was maintained at 20 to 26 °C, daily temperature changes were kept below 4 °C, and relative humidity was maintained at 40 to 60%. Neonatal mice were euthanized by physical means and adult mice by CO_2 inhalation, both in accordance with IACUC guidelines.

Mouse primary keratinocytes

Primary epidermal keratinocytes were isolated from the skin of one-day-old neonatal C57BL/6 mice. The skin was removed as a single sheet and incubated overnight at 4 °C in 0.25% trypsin. The epidermis and dermis were then mechanically separated using forceps, and the epidermal cells were gently scraped off. The collected cells were centrifuged and resuspended in minimum essential medium (MEM) supplemented with 1.3 mM calcium. The cell suspension was passed through a 100 μm cell strainer, centrifuged again, and then seeded onto plates in 10% MEM medium. All animal procedures were conducted in accordance with protocols approved by the institutional animal care and use committee.

Generation of STS TG and STS KO mice

To generate STS transgenic mice, a 7,088-bp fragment of the human STS gene, including the CMV promoter, was synthesized and inserted into the AmpR site of the pcDNA3.1 vector, creating the STS plasmid for microinjection. The plasmid was digested with PvuI and AvrII restriction enzymes, removing the 4.4-kb backbone fragment and isolating the desired 2.2-kb fragment via gel extraction. This STS DNA was injected into the male pronucleus of zygotes, which were transferred into the oviducts of pseudopregnant female mice. After the F0 generation was born, genotyping was performed using PCR on tail samples to confirm the presence of the STS gene, with a

forward primer specific to the CMV promoter and a reverse primer for the human STS gene. For the generation of STS KO mice, a Cas9 targeting vector was constructed, incorporating guide RNAs (gRNAs) designed to induce double-strand breaks (DSBs) in the Cas9 gene, alongside a selectable marker such as the puromycin resistance gene. This vector was introduced into embryonic stem (ES) cells via PEG-mediated transfection, and the transfected cells were cultured under puromycin selection to isolate cells that incorporated the targeting vector. Successful targeting events were confirmed using PCR and Southern blot analysis, with PCR primers amplifying regions surrounding the Cas9 gene and the targeting vector, and Southern blot probes hybridizing to specific sites within the Cas9 gene. Successfully targeted ES cells were injected into blastocysts, which were transferred into pseudopregnant females to generate chimeric mice. These chimeric mice contained a mixture of cells from both the original blastocyst and the injected ES cells. All animal experiments adhered to the guidelines of the Institutional Animal Care and Use Committee at Chung-Ang University. The STS transgenic mice were maintained under pathogen-free conditions at Macrogen, Inc. (Seoul, Korea).

RNA-seq

Skin tissue samples from 8-week-old male mice were used for RNA-seq. Total RNA was extracted and processed to prepare libraries using the NEB Next Ultra II Directional RNA-Seq Kit (New England Biolabs, UK). Poly(A) RNA was isolated with the Poly(A) RNA Selection Kit (Lexogen, Austria), and the resulting mRNA was used for cDNA synthesis and shearing according to the manufacturer's instructions. Illumina indexes 1–12 were utilized for sample indexing, with PCR included for enrichment. Fragment sizes were assessed using the Agilent 2100 Bioanalyzer and the DNA High Sensitivity Kit. Library quantification was performed using the Library Quantification Kit and a Step One Real-Time PCR System (Life Technologies, CA). High-throughput paired-end 100 sequencing was carried out on a HiSeq X10 sequencer (Illumina, CA).

Transcriptome analysis

Mouse skin samples were sequenced following the standard Illumina protocol (Shanghai Bingwang Biotechnology Co., Ltd.). Sequencing reads were aligned to the mouse genome (Mm9) using HISAT2 (v2.1), and gene counts were estimated with 'HTSeq.' Differential expression analysis was conducted using the 'DESeq2' R package. Genes with a fold-change > 2 and an adjusted p-value < 0.05 were considered differentially expressed genes (DEGs). GO enrichment analysis for the DEGs was performed using the 'topGO' R package, while GSEA was carried out according to the GSEA manual.

Statistical analysis

Dunnett's pairwise multiple comparison t-test was performed using the GraphPad Prism 7 software (GraphPad Software, CA). Differences were considered statistically significant at $^{*}p < 0.05$.

Data availability

The datasets generated and/or analyzed during the current study are available in the GitHub repository, https://github.com/biochem820/STS-KO-TG-RNA-seq/blob/main/STS%20KO%20TG%20seq.txt.

Received: 19 September 2024; Accepted: 26 December 2024
Published online: 21 March 2025

References

1. Reed, M. J., Purohit, A., Woo, L. W. L., Newman, S. P. & Potter, B. V. L. Steroid sulfatase: molecular biology, regulation, and inhibition. *Endocr. Rev.* **26**, 171–202. https://doi.org/10.1210/er.2004-0003 (2005).
2. Mueller, J. W., Gilligan, L. C., Idkowiak, J., Arlt, W. & Foster, P. A. The regulation of steroid action by sulfation and desulfation. *Endocr. Rev.* **36**, 526–563. https://doi.org/10.1210/er.2015-1036 (2015).
3. Pitts, R. L. Serum elevation of dehydroepiandrosterone sulfate associated with male pattern baldness in young men. *J. Am. Acad. Dermatol.* **16**, 571–573. https://doi.org/10.1016/s0190-9622(87)70075-9 (1987).
4. Bragulla, H. H. & Homberger, D. G. Structure and functions of keratin proteins in simple, stratified, keratinized and cornified epithelia. *J. Anat.* **214**, 516–559. https://doi.org/10.1111/j.1469-7580.2009.01066.x (2009).
5. Elias, P. M., Williams, M. L., Choi, E. H. & Feingold, K. R. Role of cholesterol sulfate in epidermal structure and function: lessons from X-linked ichthyosis. *Biochim. Biophys. Acta* **1841**, 353–361. https://doi.org/10.1016/j.bbalip.2013.11.009 (2014).
6. Van Scott, E. J. & Yu, R. J. Hyperkeratinization, corneocyte cohesion, and alpha hydroxy acids. *J. Am. Acad. Dermatol.* **11**, 867–879. https://doi.org/10.1016/s0190-9622(84)80466-1 (1984).
7. Zingkou, E., Pampalakis, G. & Sotiropoulou, G. Keratinocyte differentiation and proteolytic pathways in skin (patho) physiology. *Int. J. Dev. Biol.* **66**, 269–275. https://doi.org/10.1387/ijdb.210161gs (2022).
8. Lian, X. H., Yang, T. & Xiang, M. M. Roles of tissue plasminogen activator in epidermal stratification. *Colloid Surf. B* **27**, 231–240. https://doi.org/10.1016/S0927-7765(02)00077-2 (2003).
9. Vicanová, J. et al. Normalization of epidermal calcium distribution profile in reconstructed human epidermis is related to improvement of terminal differentiation and stratum corneum barrier formation. *J. Invest. Dermatol.* **111**, 97–106. https://doi.org/10.1046/j.1523-1747.1998.00251.x (1998).
10. Micallef, L. et al. Effects of extracellular calcium on the growth-differentiation switch in immortalized keratinocyte HaCaT cells compared with normal human keratinocytes. *Exp. Dermatol.* **18**, 143–151. https://doi.org/10.1111/j.1600-0625.2008.00775.x (2009).
11. Turksen, K. & Troy, T. C. Overexpression of the calcium sensing receptor accelerates epidermal differentiation and permeability barrier formation in vivo. *Mech. Dev.* **120**, 733–744. https://doi.org/10.1016/s0925-4773(03)00045-5 (2003).
12. Tu, C. L. et al. Ablation of the calcium-sensing receptor in keratinocytes impairs epidermal differentiation and barrier function. *J. Invest. Dermatol.* **132**, 2350–2359. https://doi.org/10.1038/jid.2012.159 (2012).
13. Müller, E. J., Williamson, L., Kolly, C. & Suter, M. M. Outside-in signaling through integrins and cadherins: a central mechanism to control epidermal growth and differentiation? *J. Invest. Dermatol.* **128**, 501–516. https://doi.org/10.1038/sj.jid.5701248 (2008).
14. Zhao, H. et al. The effect of γ-aminobutyric acid intake on UVB- induced skin damage in hairless mice. *Biomol. Ther. (Seoul)* **31**, 640–647. https://doi.org/10.4062/biomolther.2023.085 (2023).

15. Tu, C. L. & Bikle, D. D. Role of the calcium-sensing receptor in calcium regulation of epidermal differentiation and function. *Best Pract. Res. Clin. Endocrinol. Metab.* **27**, 415–427. https://doi.org/10.1016/j.beem.2013.03.002 (2013).
16. Tu, C. L., Chang, W., Xie, Z. & Bikle, D. D. Inactivation of the calcium sensing receptor inhibits e-cadherin-mediated cell-cell adhesion and calcium-induced differentiation in human epidermal keratinocytes. *J. Biol. Chem.* **283**, 3519–3528. https://doi.org/10.1074/jbc.M708318200 (2008).
17. Calautti, E. et al. Tyrosine phosphorylation and src family kinases control keratinocyte cell-cell adhesion. *J. Cell. Biol.* **141**, 1449–1465. https://doi.org/10.1083/jcb.141.6.1449 (1998).
18. O'Keefe, E. J., Briggaman, R. A. & Herman, B. Calcium-induced assembly of adherens junctions in keratinocytes. *J. Cell. Biol.* **105**, 807–817. https://doi.org/10.1083/jcb.105.2.807 (1987).
19. Lewis, J. E., Jensen, P. J. & Wheelock, M. J. Cadherin function is required for human keratinocytes to assemble desmosomes and stratify in response to calcium. *J. Invest. Dermatol.* **102**, 870–877. https://doi.org/10.1111/1523-1747.ep12382690 (1994).
20. Nam, M. W., Kim, C. W. & Choi, K. C. Epithelial-mesenchymal transition-inducing factors involved in the progression of lung cancers. *Biomol. Ther. (Seoul)* **30**, 213–220. https://doi.org/10.4062/biomolther.2021.178 (2022).
21. Pokutta, S. & Weis, W. I. Structure and mechanism of cadherins and catenins in cell-cell contacts. *Annu. Rev. Cell. Dev. Biol.* **23**, 237–261. https://doi.org/10.1146/annurev.cellbio.22.010305.104241 (2007).
22. Perez-Moreno, M., Jamora, C. & Fuchs, E. Sticky business: orchestrating cellular signals at adherens junctions. *Cell* **112**, 535–548. https://doi.org/10.1016/S0092-8674(03)00108-9 (2003).
23. Furukawa, F. et al. Cadherins in cutaneous biology. *J. Dermatol.* **21**, 802–813. https://doi.org/10.1111/j.1346-8138.1994.tb03294.x (1994).
24. Young, P. et al. E-cadherin controls adherens junctions in the epidermis and the renewal of hair follicles. *EMBO J.* **22**, 5723–5733. https://doi.org/10.1093/emboj/cdg560 (2003).
25. Zhao, Y., Sudol, M., Hanafusa, H. & Krueger, J. Increased tyrosine kinase activity of c-Src during calcium-induced keratinocyte differentiation. *Proc. Natl. Acad. Sci. USA* **89**, 8298–8302. https://doi.org/10.1073/pnas.89.17.8298 (1992).
26. Calautti, E., Missero, C., Stein, P. L., Ezzell, R. M. & Dotto, G. P. Fyn Tyrosine kinase is involved in keratinocyte differentiation control. *Gene Dev.* **9**, 2279–2291. https://doi.org/10.1101/gad.9.18.2279 (1995).
27. Paramio, J. M. et al. Modulation of cell proliferation by cytokeratins K10 and K16. *Mol. Cell. Biol.* **19**, 3086–3094. https://doi.org/10.1128/MCB.19.4.3086 (1999).
28. Pivarcsi, A., Szell, M., Kemeny, L., Dobozy, A. & Bata-Csorgo, Z. Serum factors regulate the expression of the proliferation-related genes alpha5 integrin and keratin 1, but not keratin 10, in HaCaT keratinocytes. *Arch. Dermatol. Res.* **293**, 206–213. https://doi.org/10.1007/s004030100217 (2001).
29. Watt, F. M. Involucrin and other markers of keratinocyte terminal differentiation. *J. Invest. Dermatol.* **81**, 100s–103. https://doi.org/10.1111/1523-1747.ep12540786 (1983).
30. Shen, C. S. et al. Premature apoptosis of keratinocytes and the dysregulation of keratinization in porokeratosis. *Br. J. Dermatol.* **147**, 498–502. https://doi.org/10.1046/j.1365-2133.2002.04853.x (2002).
31. Baek, H. S., Kwon, T. U., Shin, S., Kwon, Y. J. & Chun, Y. J. Steroid sulfatase deficiency causes cellular senescence and abnormal differentiation by inducing yippee-like 3 expression in human keratinocytes. *Sci. Rep.* **11**, 20867. https://doi.org/10.1038/s41598-021-00051-w (2021).
32. Steinert, P. M. & Marekov, L. N. The proteins elafin, filaggrin, keratin intermediate filaments, loricrin, and small proline-rich proteins 1 and 2 are isodipeptide cross-linked components of the human epidermal cornified cell envelope. *J. Biol. Chem.* **270**, 17702–17711. https://doi.org/10.1074/jbc.270.30.17702 (1995).
33. Jung, M. H., Jung, S. M. & Shin, H. S. Co-stimulation of HaCaT keratinization with mechanical stress and air-exposure using a novel 3D culture device. *Sci. Rep.* **6**, 33889. https://doi.org/10.1038/srep33889 (2016).
34. Kwon, T. U. et al. Unraveling the molecular mechanisms of cell migration impairment and apoptosis associated with steroid sulfatase deficiency: implications for X-linked ichthyosis. *Biochim. Biophys. Acta Mol. Basis Dis.* **167004** https://doi.org/10.1016/j.bbadis.2023.167004 (2024).
35. Xie, Z., Singleton, P. A., Bourguignon, L. Y. & Bikle, D. D. Calcium-induced human keratinocyte differentiation requires src- and fyn-mediated phosphatidylinositol 3-kinase-dependent activation of phospholipase C-gamma1. *Mol. Biol. Cell.* **16**, 3236–3246. https://doi.org/10.1091/mbc.e05-02-0109 (2005).
36. Zhang, M. et al. Structural basis for calmodulin as a dynamic calcium sensor. *Structure* **20**, 911–923. https://doi.org/10.1016/j.str.2012.03.019 (2012).
37. Junho, C. V. C., Caio-Silva, W., Trentin-Sonoda, M. & Carneiro-Ramos, M. S. An overview of the role of calcium/calmodulin-dependent protein kinase in cardiorenal syndrome. *Front. Physiol.* **11**, 735. https://doi.org/10.3389/fphys.2020.00735 (2020).
38. Elies, J. et al. An update to calcium binding proteins. *Adv. Exp. Med. Biol.* **1131**, 183–213. https://doi.org/10.1007/978-3-030-12457-1_8 (2020).
39. Tu, C. L., Chang, W. & Bikle, D. D. The calcium-sensing receptor-dependent regulation of cell-cell adhesion and keratinocyte differentiation requires rho and filamin A. *J. Invest. Dermatol.* **131**, 1119–1128. https://doi.org/10.1038/jid.2010.414 (2011).
40. Tsien, R. Y. A non-disruptive technique for loading calcium buffers and indicators into cells. *Nature* **290**, 527–528. https://doi.org/10.1038/290527a0 (1981).
41. Nussbaumer, P. & Billich, A. Steroid sulfatase inhibitors. *Med. Res. Rev.* **24**, 529–576. https://doi.org/10.1002/med.20008 (2004).
42. Suh, B. Y. et al. Induction of steroid sulfatase expression by tumor necrosis factor-α through phosphatidylinositol 3-kinase/Akt signaling pathway in PC-3 human prostate cancer cells. *Exp. Mol. Med.* **43**, 646–652. https://doi.org/10.3858/emm.2011.43.11.073 (2011).
43. Tu, C. L., Oda, Y., Komuves, L. & Bikle, D. D. The role of the calcium-sensing receptor in epidermal differentiation. *Cell. Calcium* **35**, 265–273. https://doi.org/10.1016/j.ceca.2003.10.019 (2004).
44. McGeoghan, F. et al. RNA sequencing and lipidomics uncovers novel pathomechanisms in recessive X-linked ichthyosis. *Front. Mol. Biosci.* **10**, 1176802. https://doi.org/10.3389/fmolb.2023.1176802 (2023).
45. Tu, C. L. & You, M. Obligatory roles of filamin A in e-cadherin-mediated cell-cell adhesion in epidermal keratinocytes. *J. Dermatol. Sci.* **73**, 142–151. https://doi.org/10.1016/j.jdermsci.2013.09.007 (2014).
46. Wheelock, M. J. & Johnson, K. R. Cadherin-mediated cellular signaling. *Curr. Opin. Cell. Biol.* **15**, 509–514. https://doi.org/10.1016/s0955-0674(03)00101-7 (2003).

Author contributions

T. U. Kwon designed and conducted the study; T. U. Kwon, Y. J. Kwon, H. Park, and Y. J. Kang analyzed the data; and T. U. Kwon and Y. J. Chun wrote the manuscript.

Funding

This research was supported by the National Research Foundation of Korea (NRF), funded by the Korean government (MSIP) (NRF-2021R1A2C201239514) and Chung-Ang University Research Grants in 2025. The funding agency had no role in the study design, data collection, analysis, publication decision, or manuscript preparation.

Declarations

Competing interests
The authors declare no competing interests.

Compliance with ethical standards
All animal experiments were approved by the Institutional Animal Care and Use Committee (IACUC) of Chung-Ang University (protocol numbers 2017-00096 and 2019-00003) and were conducted in accordance with the approved guidelines.

Additional information
Supplementary Information The online version contains supplementary material available at https://doi.org/10.1038/s41598-024-84701-9.

Correspondence and requests for materials should be addressed to Y.-J.C.

Reprints and permissions information is available at www.nature.com/reprints.

Publisher's note Springer Nature remains neutral with regard to jurisdictional claims in published maps and institutional affiliations.